Available online at www.sciencedirect.com

SCIENCE DIRECT®

Surface Science 586 (2005) 1–14

SURFACE SCIENCE

www.elsevier.com/locate/susc

Model car-exhaust catalyst studied by TPD and TP-RAIRS: Surface reactions of NO on clean and O-covered Ir{1 0 0}

Sabyasachi Khatua, Georg Held, David A. King *

Department of Chemistry, University of Cambridge, Lensfield Road, Cambridge CB2 1EW, UK

Received 26 January 2005; accepted for publication 23 April 2005
Available online 23 May 2005

Abstract

The adsorption of NO on Ir{1 0 0} has been studied as a function of NO coverage and temperature using temperature programmed reflection absorption infrared spectroscopy (TP-RAIRS), low energy electron diffraction (LEED) and temperature programmed desorption (TPD). After saturating the clean (1 × 5)-reconstructed surface with NO at 95 K, two N_2 desorption peaks are observed upon heating. The first N_2 peak at 346 K results from the decomposition of bridge-bonded NO, and the second at 475 K from the decomposition of atop-bonded NO molecules. NO decomposition is proposed to be the rate limiting step for both N_2 desorption states. For high NO coverages on the (1 × 5) surface, the narrow width of the first N_2 desorption peak is indicative of an autocatalytic process for which the parallel formation of N_2O appears to be the crucial step. When NO is adsorbed on the metastable unreconstructed (1 × 1) phase of clean Ir{1 0 0} N_2 desorption starts at lower temperatures, indicating that this surface modification is more reactive. When a high coverage of oxygen, near 0.5 ML, is pre-adsorbed on the surface, the decomposition of NO is inhibited and mainly desorption of intact NO is observed.

Keywords: Iridium; Single crystal surfaces; Nitrogen oxide; Oxygen; Nitrogen; Surface chemical reaction; Thermal desorption spectroscopy; Infrared absorption spectroscopy

1. Introduction

The catalytic conversion of NO_x species to N_2 and O_2 in car exhaust gases has recently received growing interest in connection with the challenge posed by lean-burn engines [1,2]. These engines operate with a higher oxygen content in the

---

[*] Corresponding author. Tel.: +44 1223 336449; fax: +44 1223 762829.
E-mail address: dak10@cam.ac.uk (D.A. King).

0039-6028/$ - see front matter © 2005 Elsevier B.V. All rights reserved.
doi:10.1016/j.susc.2005.04.045

combustion mixture than conventional engines. As a consequence, there is excess oxygen in the exhaust gas which makes the reduction of NO_x species thermodynamically less favourable and tends to poison most platinum-metal catalysts. Iridium-based catalysts were found to be among those able to selectively perform this reaction under oxygen-rich conditions when small quantities of hydrocarbons are present in the reaction gas mixture [3–6]. Many fundamental questions concerning this process are, however, still unsolved, for instance the origin of the catalyst poisoning by excess oxygen or the exact nature of the elementary surface reaction steps. These questions were addressed recently in a detailed theoretical study by Liu et al. [6] for NO oxidation/reduction on the Ir{1 1 1} and {2 1 1} surfaces, identifying oxidation of the Ir substrate and a lower activation barrier towards NO_2 formation as the key limiting factors for NO reduction under oxygen-rich conditions. There is, however, a need for further experimental evidence to support these findings.

The adsorption of NO on metal surfaces has been the subject of a large number of surface science experiments in recent years because of its profound importance in many fields of science and technology [7]. Due to its relatively low dissociation energy of 630 kJ/mol, NO is more susceptible to dissociation than CO, which has a dissociation energy of 1076 kJ/mol [8]. Both molecular and dissociative adsorptions of NO are observed on many transition metal single crystals. This topic has been reviewed recently by Brown and King [7]. As a consequence of the dissociative adsorption, a variety of surface species such as NO_2, N_2O, $(NO)_2$ and N and O adatoms have been found on transition metal surfaces under different reaction conditions. Apart from the competition between molecular and dissociative adsorption, the situation becomes even more complex when the surface topology changes during adsorption, as for Ir{1 0 0}. The most stable structure of the clean surface is the (1×5) quasi-hexagonal reconstruction, which can be lifted by the adsorption of CO or NO at relatively low temperatures [9,10]. An earlier study of NO adsorption on Ir{1 0 0} by Gardner et al. using high resolution electron energy loss spectroscopy (HREELS), reflexion absorption IR spectroscopy (RAIRS), temperature programmed desorption (TPD), and low energy electron diffraction (LEED), has shown that there is a close correlation between the substrate structure and the decomposition of NO [11]. The present study concentrates on the reaction mechanisms and kinetics of the different decomposition steps occurring on this surface. A detailed discussion of adsorption energies and the assignment of bands in the RAIR spectra on the basis of density functional theory (DFT) calculations will be published separately [12].

2. Experimental procedures

The experiments were performed in an UHV chamber at a base pressure of about 2×10^{-10} mbar. Details of sample preparation and experimental conditions are described elsewhere [9,10,12–15]. In brief, the sample was cleaned by Ar ion sputtering at 900 K, annealing at 1400 K, oxygen treatment at 1160 K and finally flashing to 1400 K. This procedure produces a sharp (1×5) LEED pattern with low background intensity, indicating a well ordered surface. In order to prepare the metastable (1×1) phase, the surface was first exposed to 20 L of oxygen at 475 K and then annealed to 750 K, which lifts the reconstruction completely. Oxygen was then titrated off by dosing 30 L of CO at room temperature. The remaining CO was removed by heating the sample again to 750 K, which produces a sharp (1×1) LEED pattern.

Temperature programmed reflection absorption infrared spectroscopy (TP-RAIRS) [16] was used as the principal technique of investigation supplemented by LEED and TPD. All TP-RAIR spectra were recorded continuously through a computer programme at $4\,\mathrm{cm}^{-1}$ resolution and presented as a ratio against clean surface spectra, also obtained during temperature ramping. In all TPD and TP-RAIRS experiments, the temperature was ramped linearly at $2\,\mathrm{K\,s}^{-1}$; the spectra are presented as raw data unless otherwise stated. TPD and TP-RAIR spectra were recorded simultaneously on two separate computers. Each RAIR spectrum takes 15 s to record plus 1 s to reinitialise the spectrometer. During this time the crystal temperature rises by 32 K, which is used to make a correlation between the TPD and the TP-RAIR spectra. The temperature assigned to each TP-RAIR spectrum in the figures below indicates the temperature at the end of the data collection, i.e. the corresponding spectrum covers the temperature range of 30 K below the indicated value.

In all TPD spectra of mass 28 (CO or N_2) and 30 (NO), peaks were observed at around 110 K. Since these peaks are attributed to desorption from the heating wires, the temperature range below 150 K in the TPD spectra is not discussed here.

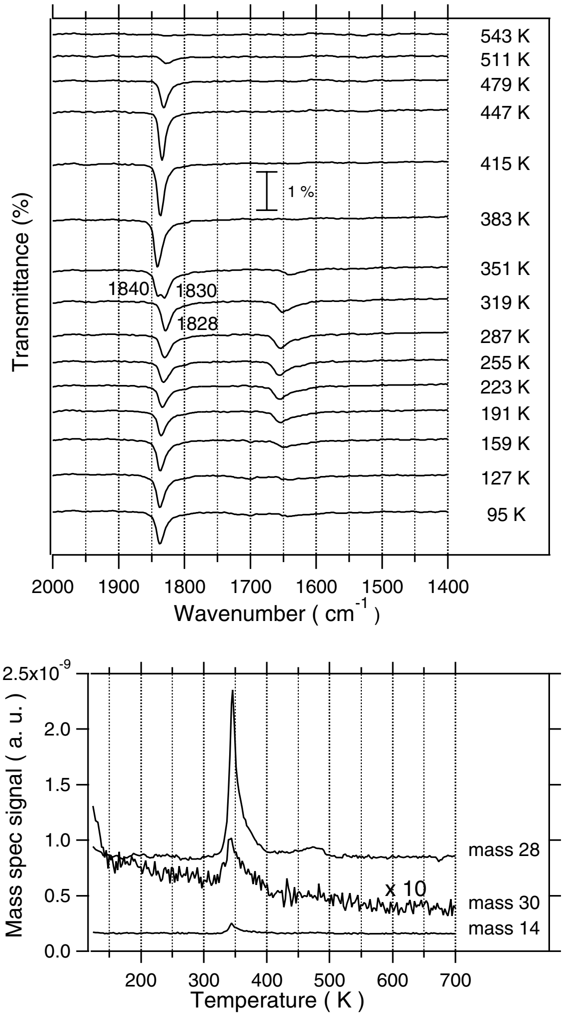

Fig. 1. TP-RAIR (top) and TPD spectra for masses 14, 28, and 30 (bottom) following the adsorption of 6.3 L (0.5 ML) ^{14}NO on the Ir{1 0 0} (1 × 5)-reconstructed surface at 95 K (heating rate 2 K s^{-1}; the temperature indicated next to each RAIR spectrum refers to the end of the data collection).

3. Experimental results

3.1. *TPD and TP-RAIR spectra from NO adsorbed on the (1 × 5) phase*

Fig. 1 shows TPD and TP-RAIR spectra recorded after the initially clean (1 × 5) surface was exposed to 6.3 L of NO at 95 K (1 L = 10^{-6} Torr s). This corresponds to the saturation coverage of NO and causes the disappearance of the (1 × 5) superstructure spots in the LEED pattern. Instead, stripes of diffuse intensity are observed between the integer order spots, which indicates incomplete lifting of the substrate reconstruction at this low temperature. The first TP-RAIR spectrum of Fig. 1 was recorded at 95 K and the temperature ramp was started after the data collection for this spectrum had finished.

The mass 28 TPD signal starts to rise at ∼325 K and has a peak at 346 K. This peak is assigned to recombinative desorption of N_2, which is supported by the presence of a corresponding mass 14 signal. The narrow width of the N_2 desorption peak (FWHM ∼ 10 K) is indicative of an autocatalytic process [17]. Closer inspection of the mass 30 signal reveals that N_2 starts to desorb only after some NO is desorbed (NO starts to desorb from about 320 K) generating vacant sites, which seem to be essential for this autocatalytic reaction (see Section 4). Notably, the end of this first N_2 desorption peak at around 400 K coincides with the nearly total disappearance of the IR band at around 1650 cm^{-1}, which occurs between 351 and 383 K. This band has been assigned to NO adsorbed on bridge sites [12]. Therefore, this N_2 desorption feature is attributed to the dissociation of the bridge-bonded NO molecules initiated by the availability of vacant sites after the desorption of some NO. The ratio between the integrated area under this desorption peak and the area under the remaining features in the TPD spectrum is much bigger than the ratio between the integrated intensities of the bridge-band and the band in the 1815–1850 cm^{-1} region, which is assigned to NO on atop sites [12]. Such intensity differences, usually caused by differences in the dynamic dipole moment for different adsorption sites, are, however, not unusual. For example, in the case of CO on Pt{1 1 1} the intensities of the bridge-band and the atop band differ by a factor of 5 for similar coverages [18]. Above 200 K the intensity of the bridge band increases slightly in conjunction with a simultaneous reduction in intensity of the atop band. This indicates some diffusion from atop to bridge sites with a barrier that the NO molecules can overcome above 200 K.

Between 319 and 351 K, the atop band splits and two peaks are observed, at 1830 and 1840 cm^{-1}. Above 351 K, only the 1840 cm^{-1} peak is observed and its width is narrowed considerably. This and the blue shift in the frequency indicate the formation of a dilute NO phase, presumably, due to the repulsive interaction with oxygen adatoms from the decomposition of the bridge-bonded NO.

In a separate experiment where a smaller amount of only 1.3 L NO was dosed at an ambient pressure of 2.0×10^{-9} mbar such a blue shift in the atop band was not observed. Instead, the band gradually shifted to a lower frequency before it disappeared. Therefore, the 1830 cm^{-1} band in the 351 K spectrum, which is at the same frequency as the atop band for lower temperatures, is most likely due to NO molecules in a more dispersed phase between the islands.

A second peak in the TPD spectrum of mass 28 is observed at about 475 K. Since the intensity of the atop band in RAIRS decreases drastically between 447 K and 511 K, this peak can be assigned to recombinative N_2 desorption resulting from the dissociation of the remaining NO molecules on atop sites. The corresponding mass 14 signal in this temperature range cannot be resolved from the noise due to its low intensity. Since each NO molecule, which dissociates to produce N_2 around 350 K leaves an O atom on the surface, the O atom coverage is relatively high during this process. With further increase in temperature oxygen (O_2) desorbs above 860 K (not shown in Fig. 1).

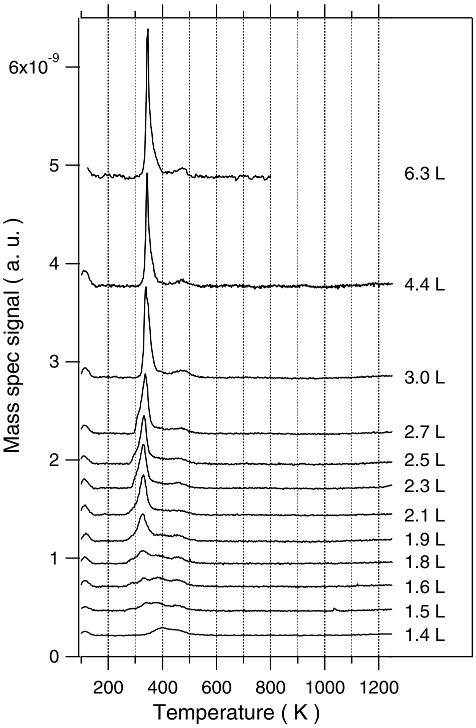

Fig. 2. TPD spectra for mass 28 (N_2 desorption) for different exposures of NO on the Ir{1 0 0} (1 × 5)-reconstructed surface (heating rate 2 K s^{-1}).

Fig. 2 shows a set of N_2 desorption traces (mass 28) as a function of NO exposure at 95 K. Before recording each set of data, the crystal was cleaned through a complete cleaning cycle as described in the experimental section. The indicated dose of NO was then adsorbed onto the clean (1 × 5) surface at 95 K followed by the TPD experiment using a heating rate of 2 K s^{-1}. Two peaks are observed in most cases. Only in the exposure range 1.5–2.0 L (0.2 ± 0.05 ML) four desorption features between 290 and 500 K can be resolved. In the lowest exposure (1.4 L/ 0.1 ML) experiment, desorption starts at around 350 K and the first desorption peak appears at 400 K. With increasing exposure, the onset of desorption gradually shifts downwards to about 290 K (1.9 L) before shifting up to 320 K at higher exposures where NO dissociation takes place in an autocatalytic manner.

The integral over these TPD spectra has been used to find a correlation between the NO exposure and the absolute NO coverage. Oxygen adatoms left on the surface after decomposition of a saturated NO layer (6.3 L) exhibit a sharp p(2 × 1) LEED pattern at room temperature. Since the ideal O coverage of this overlayer is 0.5 ML, the saturation NO coverage prior to dissociation, as well as the total N_2 desorption signal, is taken as 0.5 ML. Thus, the total area under the N_2 desorption spectrum from any given NO exposure can be used to determine the absolute coverage by calibrating this area with respect to the saturation coverage experiment. We note, however, that oxygen is known to form p(2 × 1) islands already at lower coverage than 0.5 ML. Therefore coverages determined in this way must be considered as an upper limit.

The total area under each desorption spectrum after background subtraction is measured and plotted vs exposure in the top part of Fig. 3. Since the desorption signal does not return to zero between the peaks, it is difficult to determine the area under each peak separately. This is only done for the low-temperature desorption peak below about 380 K (lower part of Fig. 3) The end point of the steep slope of the first peak is taken as the upper integration limit for determining this area (note that on a bigger scale even the low exposure experiments clearly show two distinct peaks). This cuts off some of the tail of the low-temperature peak and its area is therefore slightly underestimated.

In both diagrams of Fig. 3 breaks in the almost linear rise of the uptake (TPD area) are observed after an exposure of about 2.8 L (0.3 ML). On the basis of LEED observations this exposure was identified as the minimum needed to partially lift the (5 × 1) reconstruction at 95 K [12]. This implies that the sticking probability of NO on the unreconstructed (1 × 1) surface is smaller than on the (1 × 5) reconstructed phase, which is in accordance with the findings on Pt{1 0 0}. There the initial sticking probabilities on the reconstructed 'hex' and the (1 × 1) phases were measured as 0.86 and 0.68 respectively [19].

3.2. Isotopically labelled NO on Ir{1 0 0}-(1 × 5)

Experiments with isotopically labelled ^{15}NO have been performed in order to elucidate the reaction mechanism of NO decomposition on the reconstructed Ir{1 0 0}-(1 × 5) surface.

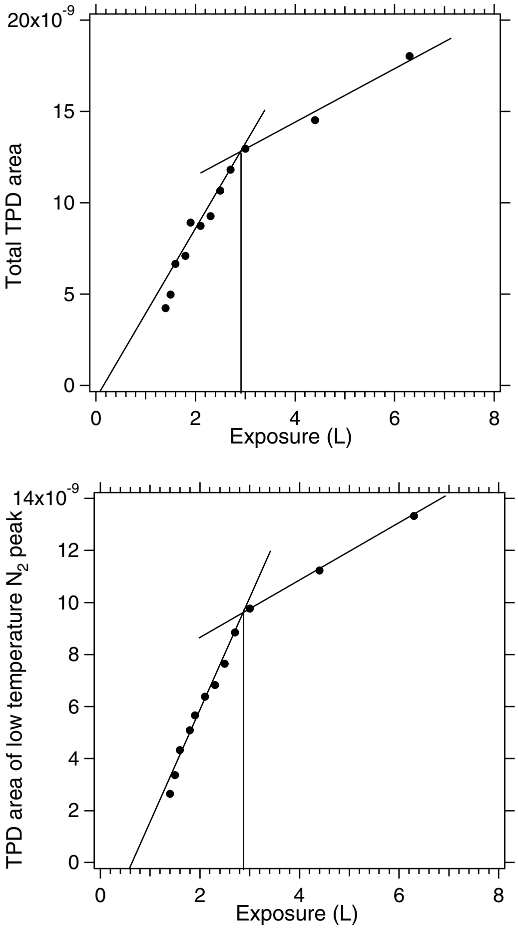

Fig. 3. Top: Plot of total N_2 TPD area as a function of total NO exposure onto Ir{1 0 0}-(1 × 5) at 95 K. Bottom: Plot of TPD area of the low-temperature N_2 desorption peak as a function of total NO exposure.

Fig. 4 shows the TP-RAIR and TPD spectra, which were recorded after the initially clean (1 × 5) surface was exposed to 6.3 L of ^{15}NO at 95 K. Large peaks are observed at 334 K in the TPD spectra of masses 30 and 15 alongside with smaller peaks at about 468 K. These features are obviously due to recombinative desorption of $^{15}N_2$. The TP-RAIRS spectra are very similar to those for ^{14}NO (cf. Fig. 1) except for a red-shift of about 4 cm^{-1}, as expected from the difference in the reduced mass. Surprisingly, however, for

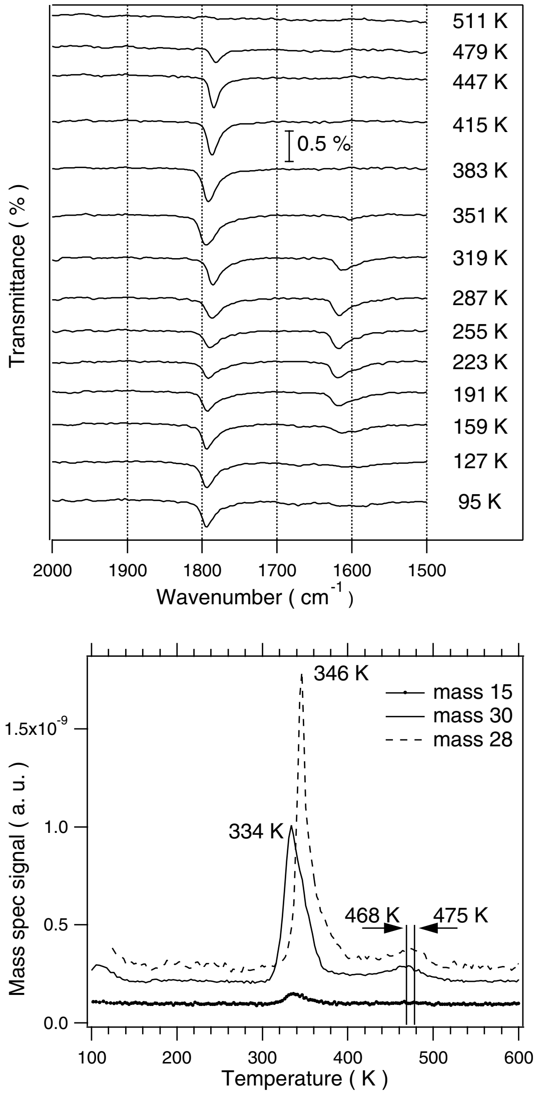

Fig. 4. Top: TP-RAIR spectra following the adsorption of 6.3 L (0.5 ML) ^{15}NO on the Ir{100} (1 × 5)-reconstructed surface at 95 K. The temperature indicated next to each RAIR spectrum refers to the end of the data collection. Bottom: Corresponding TPD spectra for masses 15 and 30. Also shown is the $^{14}N_2$ desorption spectrum (mass 28, dashed line, cf. Fig. 1) after adsorption of ^{14}NO (heating rate 2 K s^{-1} for both spectra).

an identical exposure (6.3 L) of ^{14}NO, the $^{14}N_2$ desorption peaks appear at 346 K and 475 K (also plotted in the bottom part of Fig. 4). This downshift by 12 K is very large for a kinetic isotope effect, in particular since isotope effects due to changes in the zero point energies should cause the onset of dissociation/desorption for the heavier isotope to be shifted up and not down in temperature. Small differences in the exposure can also not account for this difference. One mechanism that could explain such an unusual downshift is a better energy transfer mechanism between substrate and the adsorbate for ^{15}NO which favours dissociation at lower temperatures. This could be caused by a better energy overlap between the substrate phonon modes and the frustrated translation and rotation modes which are lower in energy for ^{15}NO than for ^{14}NO. The role of frustrated translational motion of NO in explaining some experimental results has been discussed in the literature [20,21]. Jigato et al. [20] have shown that the temperature dependence of near edge X-ray absorption fine structure (NEXAFS) data of NO/Pd{1 1 0} can be explained only by considering the frustrated translational motion of NO.

Fig. 5 shows TP-RAIR and TPD spectra, which were recorded after the clean (1 × 5) surface had been exposed to a relatively small dose of ~1.3 L of a 1:1 mixture of ^{14}NO and ^{15}NO at 95 K. Signals for masses 28, 29 and 30 are observed in TPD, which represent $^{14}N_2$, $^{14}N^{15}N$ and $^{15}N_2$ desorption traces, respectively. The ratio of the integrated TPD areas of these peaks is 1:1.9:1.1, very similar to the 1:2:1 ratio expected for recombinative desorption. The ^{14}NO and ^{15}NO peaks in the RAIR spectra do not show 1:1 intensity ratios. Instead they are dominated by the higher frequency signals of ^{14}NO due to ‘intensity stealing’ [22]. IR bands are observed in the atop and bridge regions which show similar characteristics to the ^{14}NO and ^{15}NO spectra for higher exposure (cf. Figs. 1 and 4). The decay of the IR signal above 351 K coincides with the desorption of dinitrogen from the surface.

3.3. Evidence of N_2O formation

N_2O and NO_2 are often found as byproducts of NO reactions on transition metal surfaces. In order to check for these byproducts, desorption traces of mass 44 ($^{14}N_2O$) and mass 46 ($^{14}NO_2$) were recorded after dosing 6.3 L of ^{14}NO on the

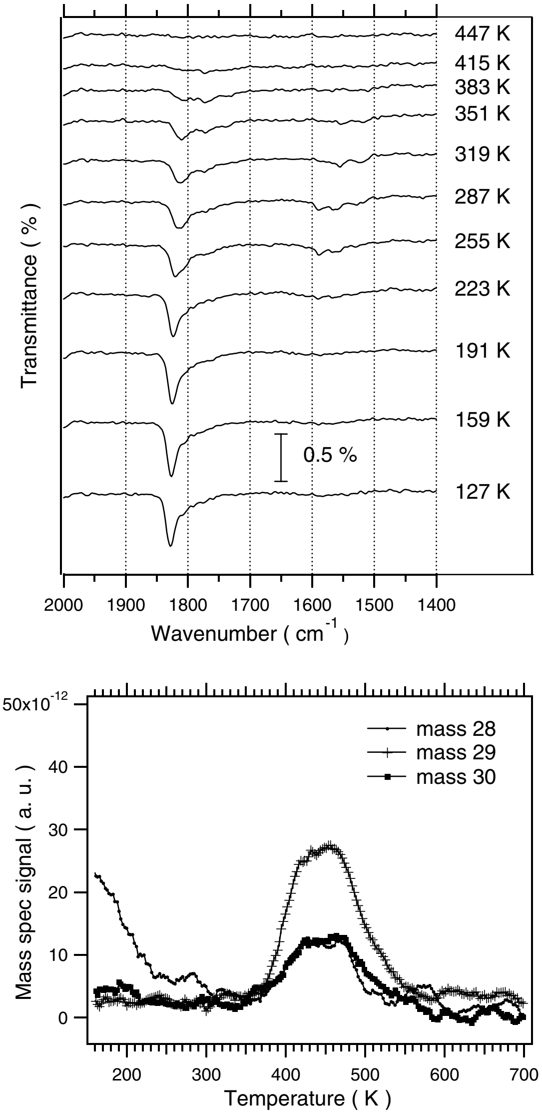

Fig. 5. TP-RAIR (top) and TPD spectra for masses 28, 29, and 30 (bottom) following the adsorption of 1.3 L (0.15 ML) of a 1:1 mixture of ^{14}NO and ^{15}NO on the Ir{100} (1 × 5)-reconstructed surface at 95 K (heating rate 2 K s^{-1}; TPD spectra are smoothed by averaging over 11 points; the temperature indicated next to each RAIR spectrum refers to the end of the data collection).

(1 × 5) surface at 95 K. No desorption signal is observed for mass 46 up to 800 K (not shown) but a small peak around 340 K is found for mass 44. This could be either be due to N_2O or CO_2. Since there is a close correlation between this peak and the N_2 desorption signal, as can be seen in Fig. 6, N_2O is the more likely origin of the mass 44 peak. N_2O starts to desorb at the same time when N adatoms are generated through the dissociation of NO. In the IR spectra, however, there is no band observed that could be related to N_2O, which indicates prompt desorption of the surface reaction product as it is formed at 340 K. Two possible pathways for N_2O formation are:

$$N_{(ad)} + NO_{(ad)} \rightarrow N_2O_{(gas)} \tag{1}$$

and

$$\begin{aligned} NO_{(ad)} + NO_{(ad)} &\rightarrow (NO)_{2(ad)} \\ &\rightarrow N_2O_{(gas)} + O_{(ad)} \end{aligned} \tag{2}$$

Since the leading edge of the N_2O desorption trace coincides exactly with that for N_2 we conclude that both N_2O and N_2 formation depend on the N adatom coverage, and that reaction (1) is the more likely pathway. In addition, it has been shown in mixed isotope experiments that no $(NO)_2$ dimers are formed on the surface [12]. Despite the fact that the N_2O and the N_2 desorption traces start simultaneously their shapes are very different. The N_2O peak temperature is 5 K lower and the peak is symmetrical whereas N_2 desorption continues up to about 500 K. This behaviour provides valuable information regarding the reaction mechanism causing the first N_2 desorption state, which will be discussed in detail in Section 4.

3.4. NO adsorbed on the unreconstructed (1 × 1) surface

Fig. 7 shows the TPD and the TP-RAIR spectra for NO adsorbed on the clean unreconstructed surface. The (1 × 1) surface, prepared as described earlier in the experimental section, was exposed to 10 L NO at 95 K, which is enough to saturate the surface. The onset of N_2 desorption (mass 28) is at about 270 K, 60 K lower than on the (1 × 5) surface. Two N_2 desorption peaks, around 310 K and 360 K, are observed along with a broad shoulder extending up to 500 K. Desorption of intact NO is not observed.

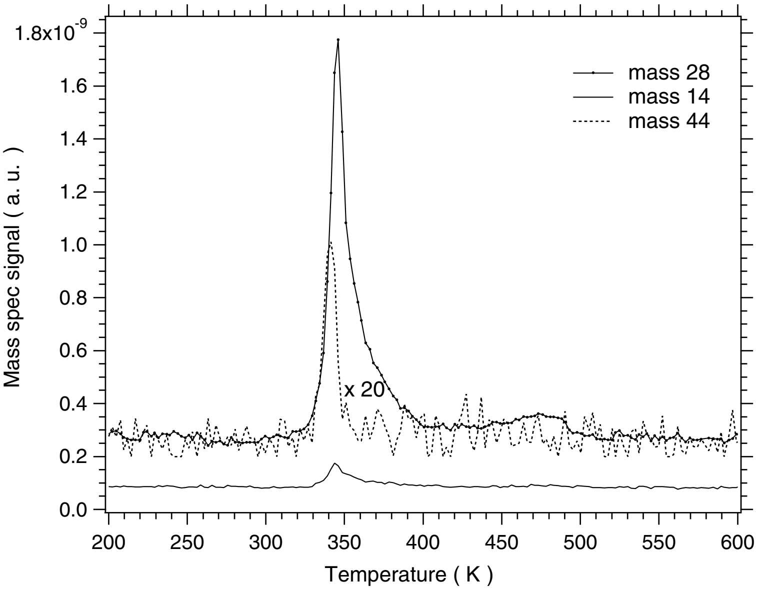

Fig. 6. TPD spectra for masses 14 (N), 28 (N_2), and 44 (N_2O) following the adsorption of 6.3 L (0.5 ML) ^{14}NO on the Ir{1 0 0} (1 × 5)-reconstructed surface at 95 K (heating rate 2 K s^{-1}).

In TP-RAIRS, two bands are observed at frequencies close to those observed on the reconstructed surface, but with the intensity ratio reversed (see Fig. 1). The band in the 1650 cm^{-1} region is assigned to adsorption on bridge sites, the one in the 1800–1850 cm^{-1} region to adsorption on atop sites. (Details of the band assignment and the energetics of NO adsorption are given in Ref. [12].) The bridge band dominates the spectra up to 287 K and only as the N_2 desorption is well under way at around 319 K is the atop band stronger. Interestingly, the spectra for 319 K in Figs. 1 and 7 are very similar indicating that the local environment of NO is the same on both surfaces at this temperature. This implies that the reconstruction of the initially hex-reconstructed surface is not complete below 319 K.

3.5. NO adsorbed on the oxygen-covered surface

In order to study the influence of a high oxygen coverage on NO dissociation, NO was adsorbed on an Ir{1 0 0} surface pre-covered by about 0.5 ML O. Following the procedure given in Ref. [11], the oxygen-covered surface was prepared by adsorbing a saturated layer of NO on the clean unreconstructed (1 × 5) surface at 95 K followed by annealing to 800 K. As a result of the annealing step, all N adatoms are removed from the surface leaving behind close to 0.5 ML O adatoms, which are arranged in a well-known p(2 × 1) structure at room temperature [23,24]. Onto this surface 6.3 L of NO is dosed again at 95 K and TPD and the TP-RAIR spectra are recorded simultaneously; these are shown in Fig. 8.

The first spectrum of the TP-RAIRS series is recorded at a constant temperature of 95 K. After the data collection for this spectrum was finished, the temperature ramp was started. In addition to the atop and bridge bands already observed for pure NO, a new band is observed at 1930 cm^{-1}, which is assigned to a NO^+ species [12]. This band disappears completely between 127 K and 159 K, accompanied by a shift of the bridge band from 1662 cm^{-1} to 1678 cm^{-1}. At 319 K this band shifts further up in frequency to 1695 cm^{-1} and shifts down again for higher temperatures. An atop band at 1844 cm^{-1} is observed between 351 K and 415 K. Above 415 K both bands disappear.

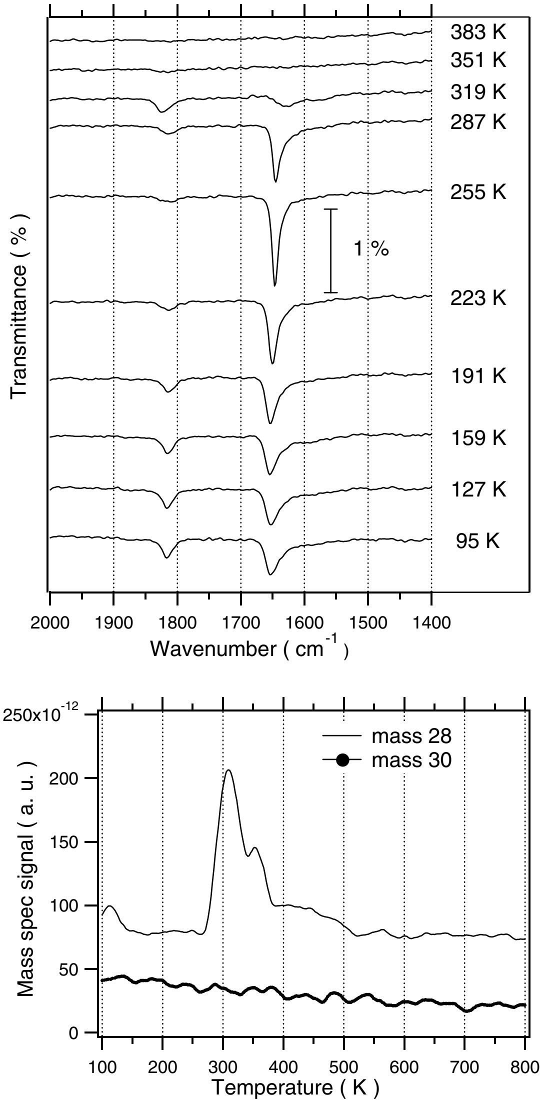

Fig. 7. TP-RAIR (top) and TPD spectra for masses 28 and 30 (bottom) following the adsorption of 10 L ^{14}NO on the metastable Ir{1 0 0} (1×1) surface at 95 K. The heating rate is 2 K s^{-1}; the temperature indicated next to each RAIR spectrum refers to the end of the data collection. The TPD spectra are smoothed by averaging over 11 points.

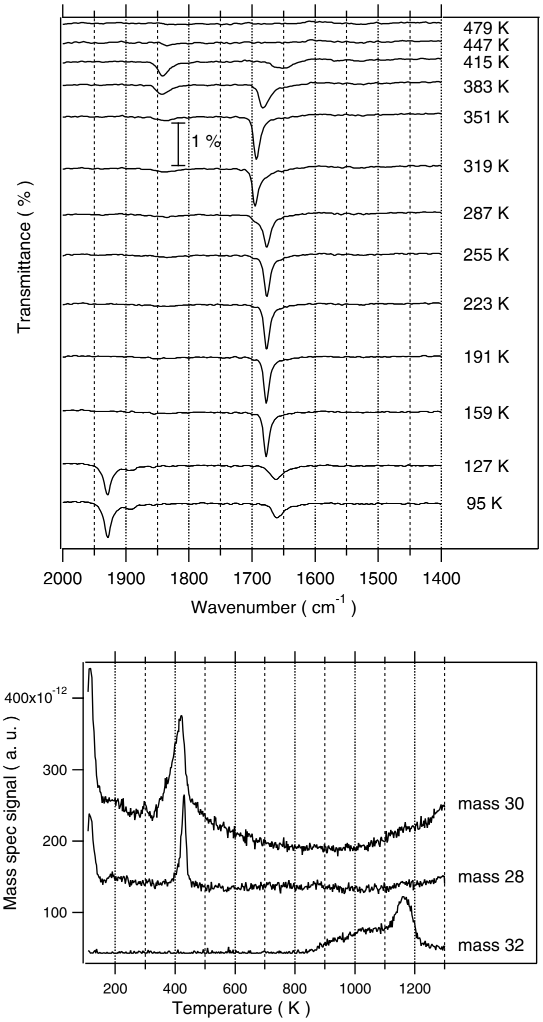

Fig. 8. TP-RAIR (top) and TPD spectra for masses 28, 30, and 32 (bottom) following the adsorption of 6.3 L ^{14}NO on an oxygen-covered Ir{1 0 0} surface at 95 K (heating rate 2 K s^{-1}; the temperature indicated next to each RAIR spectrum refers to the end of the data collection). See text for more details.

In contrast to our previous experiments on modifications of clean Ir{1 0 0}, the main desorbing species is now NO (mass 30). In the TPD spectrum of mass 30 a small NO desorption peak is observed around 300 K, which coincides with the blue shift to 1695 cm^{-1} in the bridge band. The onset of the main NO desorption peak is at 320 K, and the peak temperature is 421 K. A small amount of N_2 (mass 28) begins to desorb around 390 K, well after the onset of NO desorption. The peak temperature of the N_2 desorption signal is 430 K. Oxygen desorption (mass 32) is observed between ~860 K and ~1220 K with a peak at 1170 K and a broad shoulder at lower temperatures. No desorption of N_2O or NO_2 was observed.

4. Discussion

4.1. NO on the (1 × 5) phase of Ir{1 0 0}

It is evident from the data presented in this work that the process of NO decomposition on the (1 × 5) reconstructed Ir{1 0 0} surface takes place in two stages. In the first stage, the bridge-bonded NO molecules dissociate causing the sharp N_2 desorption peak at 346 K. The second stage, between about 440 K and 500 K, is due to the dissociation of the remaining atop-bonded molecules, which are at that stage co-adsorbed with O adatoms resulting from the first dissociation step.

The bridge band in the IR spectra of Fig. 1 disappears between 319 K and 351 K. In the temperature range above 300 K the surface also undergoes a long-range transformation into the unreconstructed (1 × 1) phase [11], which is more reactive than the (1 × 5) phase with respect to the dissociation of NO. The resulting N adatoms desorb immediately as N_2 whereas the O atoms stay on the surface and desorb recombinatively above 860 K. For higher NO coverages above about 0.2 ML (1.6 L, cf. Figs. 2 and 3), the first dissociation/desorption step occurs over a very narrow temperature range indicating an autocatalytic reaction mechanism.

The remaining atop-bonded NO molecules dissociate in the second stage. The intensity of the atop band in the IR spectra starts to decrease above 447 K and disappears completely between the 511 K and the 543 K spectra of Fig. 1. When the atop-bonded molecules dissociate there is already a significant coverage of oxygen atoms left from the decomposition of the bridge-bonded NO molecules. The N adatoms formed during this dissociation process desorb again immediately as N_2 around the peak temperature of 475 K with a desorption tail continuing up to 510 K. Notably, this peak temperature does not shift significantly with varying NO exposure, which must mean that the amount of co-adsorbed oxygen from the earlier dissociation of bridge-bonded NO has little influence. The frequency of the atop band ($1851\ \mathrm{cm}^{-1}$) is very close to the gas phase NO stretch ($1876\ \mathrm{cm}^{-1}$, [25]), although this band is observed up to relatively high temperatures, which implies a strong bond to the surface.

As outlined before, the narrow width of the peak around 346 K points towards an explosive, autocatalytic mechanism causing the desorption of N_2 at this temperature [17] and it is worthwhile examining possible rate determining steps for this process. One is the *phase transition of the substrate*. It has been mentioned earlier that after an exposure of 2.8 L (0.3 ML) NO the (5 × 1) reconstruction is partially lifted even at 95 K. In an earlier study of NO adsorption on Ir{1 0 0} at 300 K Gardner et al. [11] showed that lifting of the reconstruction starts once a critical NO coverage is reached. The diffuse LEED pattern after NO adsorption at low temperatures indicates that the reconstruction is only partially lifted, but as the temperature rises, long-range reordering starts and this change in surface topology could trigger the N_2 desorption process. However, since the RAIRS signal from intact NO is not reduced in intensity right up to the N_2 desorption peak, NO does not decompose at lower temperatures. Involvement of adsorbed NO in the rate determining step is also consistent with the peak temperature in the ^{15}NO experiment (334 K) being different from the ^{14}NO experiment (346 K). This difference can only be related to the adsorbate and not to the substrate. In conclusion, the substrate phase transformation does not appear to be the rate limiting step. The comparison of TPD spectra from the unreconstructed and initially reconstructed surface (Figs. 1 and 7) shows, however, that the state of the substrate surface has a significant influence on the reaction kinetics.

Since the RAIRS signal from intact NO is observed up to the N_2 desorption peak at 346 K, we exclude the recombination step,

$$N_{(ad)} + N_{(ad)} \rightarrow N_{2(gas)}$$

as rate determining, which leaves us with the dissociation of NO as the most likely rate determining step:

$$NO_{(ad)} \rightarrow N_{(ad)} + O_{(ad)}$$

In addition to our RAIRS data, support for this assumption also comes from the HREELS data of NO adsorption on Ir{1 0 0}-(1 × 5) at 300 K in the work by Gardner et al. [11]. At this temperature no evidence of chemisorbed oxygen or pseudo-oxide was found, therefore no appreciable NO dissociation takes place on the initially (1 × 5)-reconstructed surface. The dissociation step on this surface occurs at higher temperatures, where the transformation to (1 × 1) is still incomplete. However, as we show, on the metastable unreconstructed surface N_2 begins to desorb already around 270 K (Fig. 7).

Finally, the desorption of N_2O (Fig. 6) also fits very well into this picture. Since N_2O forms by the direct reaction of N adatoms and NO, the simultaneous onset of both N_2 and N_2O desorption at ~325 K is triggered by the availability of N adatoms at the surface. When NO starts to dissociate, both N adatoms and undissociated NO molecules are simultaneously present on the surface and hence N_2 and N_2O can form. The rapid drop of the N_2O signal after reaching its maximum, which coincides with a change in slope of the N_2 peak, marks the point at which all bridge-bonded NO has decomposed and the rate of N_2 desorption becomes determined by the recombination of N adatoms.

The surface reactions taking place at around 346 K are:

$$\begin{aligned}&\mathrm{NO}_{(\mathrm{ad,b})} + * \rightarrow \mathrm{N}_{(\mathrm{ad})} + \mathrm{O}_{(\mathrm{ad})} \quad \text{(i)}\\ &\mathrm{N}_{(\mathrm{ad})} + \mathrm{N}_{(\mathrm{ad})} \rightarrow \mathrm{N}_{2(\mathrm{gas})} + 2* \quad \text{(ii)}\\ &\mathrm{NO}_{(\mathrm{ad,b})} + \mathrm{N}_{(\mathrm{ad})} \rightarrow \mathrm{N_2O}_{(\mathrm{gas})} + 2* \quad \text{(iii)}\end{aligned} \tag{3}$$

where * marks an empty site for bridge-bonded $NO_{(ad,b)}$, N, and O adsorption. N_2 formation, ((i), (ii)), requires two empty sites for the NO dissociation step (i) and leaves behind two empty sites after N_2 desorption (ii):

$$2\mathrm{NO}_{(\mathrm{ad,b})} + 2* \rightarrow \mathrm{N}_{2(\mathrm{gas})} + 2\mathrm{O}_{(\mathrm{ad})} + 2* \tag{4}$$

There is no net gain of empty sites, i.e. this reaction path is simply catalytic. N_2O formation ((i), (iii)), however, requires only one empty site to be initiated and leaves behind two empty sites when desorption (iii) has taken place:

$$2\mathrm{NO}_{(\mathrm{ad,b})} + * \rightarrow \mathrm{N_2O}_{(\mathrm{gas})} + \mathrm{O}_{(\mathrm{ad})} + 2* \tag{5}$$

The formation of N_2O results in the generation of additional empty sites, which can again catalyse the formation of N_2O; the process is, therefore, autocatalytic. The broadening of the N_2 desorption peak as soon as N_2O formation has stopped signals the termination of the autocatalytic process. At high coverages N_2O formation will be favoured, but it can take place only as long as there are undissociated NO molecules available on the surface.

The second N_2 desorption feature is related to atop-bonded NO. The higher dissociative activation energy for this species is more likely due to the adsorption site than due to the existence of co-adsorbed oxygen from the earlier dissociation/desorption step. Otherwise this feature should not exist for the lowest coverages in Fig. 2, where no oxygen is produced in a low-temperature decomposition process.

4.2. NO adsorbed on the unreconstructed Ir{100}-(1 × 1) surface

N_2 desorption from the NO-saturated (1 × 1) surface starts at about 55 K lower temperature than from the reconstructed surface (cf. Fig. 7). This shows that the (1 × 1) phase is the more reactive surface modification, which has the lower activation energy for NO dissociation. Similar to the reconstructed surface, there are two NO species present at low temperatures, on bridge and atop adsorption sites, of which the bridge-bonded NO molecules decompose first. In contrast to the reconstructed surface, however, the desorption features in N_2 TPD are much broader and do not show any sign of autocatalytic behaviour, in accordance with the fact that no N_2O desorption was observed.

The fact that there are significant differences in the TPD and TP-RAIR spectra between the reconstructed (Fig. 1) and the unreconstructed surface (Fig. 7), even up to 500 K, suggests that the long-range lifting of the reconstruction is a slow process under the influence of NO and may not be complete even at the highest temperatures, for which N_2 desorption is observed in our experiments. The partial lifting of the reconstruction at 95 K, as observed in LEED, may be an indication that an intermediate phase is formed, similar to the (1 × 3) phase found for hydrogen adsorption on

Ir{1 0 0} [26,27]. The most striking differences between the two surface modifications are seen in the temperature range below 350 K: NO decomposition and N_2 desorption starts at around 270 K on the unreconstructed surface while no decomposition/desorption is observed below about 325 K on the initially reconstructed surface. Two explanations appear likely for this behaviour. One is that the delayed onset of N_2 desorption from the initially reconstructed surface is simply caused by the difference in the dissociative activation energies between the unreconstructed surface and the intermediate reconstruction phase. The long-range lifting of the substrate reconstruction would then be a secondary process induced by the oxygen adatoms left on the surface. The alternative explanation is that at 325 K the slow long-range lifting of the intermediate reconstruction phase under the influence of NO could have produced large enough (1×1) patches on the surface with low dissociative activation energy, which triggers NO decomposition and the formation of N_2 and N_2O.

The TPD spectrum in Fig. 7 differs from the spectrum reported in the earlier work by Gardner et al. [11]. There, three N_2 desorption peaks were observed between 250 K and 400 K whereas the spectrum in Fig. 7 only shows a very small feature at around 255 K and two N_2 peaks at 310 K and 360 K; in addition, a broad shoulder extends to about 520 K. The nominal exposure of NO (in Langmuir) prior to TPD is the same in both studies, however the actual exposure can vary significantly between different experiments, which could be the reason for this discrepancy together with the different heating rates ($2\ \mathrm{K\,s^{-1}}$ in the present study vs $5\ \mathrm{K\,s^{-1}}$ in [11]).

Gardner et al. observed two NO bands for annealing temperatures up to 400 K, whereas in the present study, the bridge band has almost disappeared at 351 K. The intensity of the atop band ($1800–1850\ \mathrm{cm^{-1}}$), on the other hand, diminishes greatly but does not attenuate completely at this temperature. From a closer inspection it is evident that there is still some trace of the atop band at 351 K with intensity around ∼0.04%. This band has disappeared after heating to 383 K. These differences between the present study and Ref. [11] could be due to readsorption from the background in the latter case, where the spectra were recorded on a cold sample after annealing. In the present study background adsorption of NO can be ruled out because the TP-RAIR spectra are recorded during heating.

4.3. NO adsorbed on the oxygen pre-covered surface

When the surface is pre-covered with oxygen near saturation, most NO desorbs intact, whereas almost complete dissociation is observed from both (1×5) and (1×1) surfaces. NO reduction is therefore inhibited by the co-adsorption of oxygen. In fact, NO dissociation can be completely suppressed on Ir{1 0 0} saturated with 0.5 ML oxygen [24]. Possible reasons for this effect are strong repulsive interactions among the O and N adatoms and site blocking. Recent calorimetric and molecular beam experiments [28,29] have shown that the thermodynamically stable state of NO adsorption on Ni{1 0 0} and Pt{1 0 0} switches from dissociative to molecular above a critical coverage of 0.16 ML NO. The thermodynamic driving force favouring the molecular adsorption state was identified as the strong near-neighbour pairwise repulsive interactions between O and N adatoms after dissociation. This is supported by DFT calculations by Ge et al. [30], who identified the Pauli repulsion between oxygen 2p orbitals as the origin of this interaction.

On Ir{1 0 0} there are indications that the interaction between neighbouring oxygen atoms is attractive in one direction and repulsive in the perpendicular direction, otherwise the formation of $p(2 \times 1)$ islands below the saturation coverage of 0.5 ML O could not be explained [23]. For oxygen atoms produced by NO dissociation within the $p(2 \times 1)$ islands the highly repulsive adsorption sites are the only ones available, which means that dissociation is thermodynamically unfavourable. If the surface is not completely saturated with oxygen, as for the data shown in Fig. 8, N_2 desorption, indicating dissociation, is observed after some intact NO has desorbed generating vacant sites outside the $p(2 \times 1)$-O islands.

The NO^+ species ($1930\ \mathrm{cm^{-1}}$) observed in TP-RAIRS at low temperatures (cf. Fig. 8) has a very weak bond to the surface [12]. It is therefore likely to desorb rather than dissociate. In the TP-RAIR spectra the NO^+ species is seen to attenuate between 127 K and 159 K. However, since the low-temperature regime of our TPD spectra is dominated by desorption from the heating wires, it is difficult to resolve their desorption from the background.

4.4. Relevance to car exhaust-gas NO_x removal

The data presented in this work and in the previous work by Gardner et al. [11] show that NO is very efficiently reduced to N_2 at modest temperatures (below 500 K) on both modifications of the clean Ir{1 0 0} surface. This would make this surface a very good exhaust catalyst, in principle. The production of N_2O which accompanies the N_2 formation only takes place at low temperatures, around 346 K, and can probably be avoided by running the reaction at higher temperatures. A more serious problem, however, is the accumulation of the second reaction product, oxygen, on the surface, which suppresses NO dissociation and, hence, poisons the catalyst. Oxygen can be removed thermally only at rather high temperatures, above 860 K. This disqualifies the surface from being used as an exhaust catalyst, especially under lean-burn (oxygen-rich) conditions, unless there is a way of removing the oxygen adatoms by a secondary reaction. Reduction by carbon monoxide or hydrocarbons, as suggested earlier [4,6], is one possible solution of this problem. These reaction mechanisms have not been studied in detail, however, and will be the subject of future work.

5. Conclusion

We have studied the adsorption of NO on Ir{1 0 0} by TP-RAIRS and TPD. On the (1×5)-reconstructed surface NO adsorbs on bridge (majority) and atop sites (minority species). An exposure of 2.8 L (0.3 ML) causes the reconstruction to be lifted locally even at 95 K. Upon annealing, two N_2 desorption features are observed in TPD between 325 K and about 500 K following the decomposition of bridge and atop-bonded NO, respectively. Alongside with the recombinative desorption of N_2 also N_2O is formed, which appears crucial in explaining the autocatalytic behaviour of the first N_2 desorption peak at 346 K.

Experiments with isotopically labelled ^{15}NO show a downward-shift of the first $^{15}N_2$ desorption peak by 12 K as compared to ^{14}NO. This unusual phenomenon might be explained by resonance-enhanced energy transfer between substrate phonons and frustrated translational and rotational motions of NO, which are lower in energy, and therefore closer to the substrate phonons, for ^{15}NO.

The unreconstructed Ir{1 0 0} (1×1) surface is more reactive than the (1×5) phase. There, NO decomposition and N_2 desorption start already at around 270 K. NO dissociation is inhibited by the presence of a high coverage of oxygen on the surface. This is a result of the repulsive interaction between oxygen atoms when the local coverage exceeds 0.5 ML.

Acknowledgements

The authors acknowledge the EPSRC for supporting this study through an equipment grant. The Cambridge Commonwealth Trust (CCT) and EPSRC are acknowledged for financial supports to S.K.

References

[1] V.I. Parvulescu, P. Grange, B. Delmon, Catal. Today 46 (1998) 233.
[2] R. Burch, J.P. Breen, F.C. Meunier, Appl. Catal. B 39 (2002) 283.
[3] M. Nakatsuji, Appl. Catal. B 25 (2000) 163.
[4] C. Wogebauer, M. Maciejwski, A. Baiker, Appl. Catal. B 34 (2001) 11.
[5] C. Wogebauer, M. Maciejwski, A. Baiker, J. Catal. 205 (2002) 157.
[6] Z.-P. Liu, S.J. Jenkins, D.A. King, J. Am. Chem. Soc. 126 (2004) 10746.
[7] W.A. Brown, D.A. King, J. Phys. Chem. B 104 (2000) 2578.
[8] D.R. Lide, CRC Handbook of Chemistry and Physics, 75th ed., CRC Press, 1997.
[9] K. Heinz, G. Schmidt, L. Hammer, K. Müller, Phys. Rev. B 32 (1985) 6214.
[10] N. Bickel, K. Heinz, Surf. Sci. 163 (1985) 435.

[11] P. Gardner, R. Martin, R. Nalezinski, C.L.A. Lamont, M.J. Weaver, A.M. Bradshaw, J. Chem. Soc., Faraday Trans. 91 (1995) 3575.

[12] S. Khatua, Z.-P. Liu, D.A. King, Surf. Sci. in press, doi:10.1016/j.susc.2005.04.002.

[13] J. Küppers, H. Michel, Appl. Surf. Sci. 3 (1979) 179.

[14] T.N. Rhodin, G. Broden, Surf. Sci. 60 (1976) 466.

[15] G. Kisters, J.G. Chen, S. Lehwald, H. Ibach, Surf. Sci. 245 (1991) 65.

[16] M. Kim, S.J. Pratt, D.A. King, J. Am. Chem. Soc. 122 (2000) 2409.

[17] J. McCarty, J. Facloner, R.J. Madix, J. Catal. 30 (1973) 235.

[18] E. Schweizer, B.N.J. Persson, M. Tüshaus, D. Hoge, A.M. Bradshaw, Surf. Sci. 213 (1989) 49.

[19] Y.Y. Yeo, L. Vattuone, D.A. King, J. Chem. Phys. 104 (1996) 3810.

[20] M. Pérez Jigato, W.K. Walter, D.A. King, Surf. Sci. 301 (1994) 273.

[21] J. Singh, W.K. Walter, A. Atrei, D.A. King, Chem. Phys. Lett. 185 (1991) 426.

[22] A. Crossley, D.A. King, Surf. Sci. 68 (1977) 528.

[23] K. Johnson, Q. Ge, S. Titmuss, D.A. King, J. Chem. Phys. 112 (2000) 10460.

[24] T.J. Lerotholi, B. Russell, S.M. Driver, G. Held, D.A. King, in preparation.

[25] K.P. Huber, G. Herzberg, Molecular Spectra and Molecular Structure, IV. Constants of Diatomic Molecules, Van Nostrand Reinhold, New York, 1979.

[26] K. Moritani, M. Okada, T. Kasai, Y. Murata, Surf. Sci. 445 (2000) 315.

[27] B. Sauerhammer, K. Johnson, C. Greenwood, W. Braun, G. Held, D.A. King, Surf. Sci. 488 (2001) 154.

[28] L. Vattuone, Y.Y. Yeo, D.A. King, J. Chem. Phys. 104 (1996) 8096.

[29] J.M. Bradley, A. Hopkinson, D.A. King, J. Phys. Chem. 99 (1995) 17032.

[30] Q. Ge, D.A. King, Chem. Phys. Lett. 285 (1998) 15.